



Published in final edited form as:

*Proc SPIE Int Soc Opt Eng.* 2016 February 27; 9784: . doi:10.1117/12.2217179.

## Demons versus Level-Set motion registration for coronary $^{18}\text{F}$ -sodium fluoride PET

Mathieu Rubeaux<sup>a</sup>, Nikhil Joshi<sup>b</sup>, Marc R. Dweck<sup>b</sup>, Alison Fletcher<sup>b</sup>, Manish Motwani<sup>a</sup>, Louise E. Thomson<sup>a</sup>, Guido Germano<sup>a</sup>, Damini Dey<sup>a</sup>, Daniel S. Berman<sup>a</sup>, David E. Newby<sup>b</sup>, and Piotr J. Slomka<sup>a,\*</sup>

<sup>a</sup> Cedars-Sinai Medical Center, Los Angeles, CA, USA

<sup>b</sup> University of Edinburgh, Edinburgh, United Kingdom

### Abstract

Ruptured coronary atherosclerotic plaques commonly cause acute myocardial infarction. It has been recently shown that active microcalcification in the coronary arteries, one of the features that characterizes vulnerable plaques at risk of rupture, can be imaged using cardiac gated  $^{18}\text{F}$ -sodium fluoride ( $^{18}\text{F}$ -NaF) PET. We have shown in previous work that a motion correction technique applied to cardiac-gated  $^{18}\text{F}$ -NaF PET images can enhance image quality and improve uptake estimates. In this study, we further investigated the applicability of different algorithms for registration of the coronary artery PET images. In particular, we aimed to compare demons vs. level-set nonlinear registration techniques applied for the correction of cardiac motion in coronary  $^{18}\text{F}$ -NaF PET. To this end, fifteen patients underwent  $^{18}\text{F}$ -NaF PET and prospective coronary CT angiography (CCTA). PET data were reconstructed in 10 ECG gated bins; subsequently these gated bins were registered using demons and level-set methods guided by the extracted coronary arteries from CCTA, to eliminate the effect of cardiac motion on PET images. Noise levels, target-to-background ratios (TBR) and global motion were compared to assess image quality.

Compared to the reference standard of using only diastolic PET image (25% of the counts from PET acquisition), cardiac motion registration using either level-set or demons techniques almost halved image noise due to the use of counts from the full PET acquisition and increased TBR difference between  $^{18}\text{F}$ -NaF positive and negative lesions. The demons method produces smoother deformation fields, exhibiting no singularities (which reflects how physically plausible the registration deformation is), as compared to the level-set method, which presents between 4 and 8% of singularities, depending on the coronary artery considered.

In conclusion, the demons method produces smoother motion fields as compared to the level-set method, with a motion that is physiologically plausible. Therefore, level-set technique will likely require additional post-processing steps. On the other hand, the observed TBR increases were the highest for the level-set technique. Further investigations of the optimal registration technique of this novel coronary PET imaging technique are warranted.

\* piotr.slomka@cshs.org; phone 1 310 423 4348.

## Keywords

<sup>18</sup>F-sodium fluoride PET; demons registration; level-set registration; acute myocardial infarction; active microcalcification

---

## 1. INTRODUCTION

In recent studies<sup>1-3</sup>, it has been shown that in coronary PET imaging <sup>18</sup>F-sodium fluoride (<sup>18</sup>F-NaF) binds preferentially to regions of vascular microcalcification and that <sup>18</sup>F-NaF uptake can be used to identify high-risk plaques in the coronary arteries. In particular, Joshi et al have demonstrated that increased <sup>18</sup>F-NaF PET activity localized to exact site of plaque rupture in >90% of patients who had recently suffered AMI, independent of stenting<sup>1</sup>. <sup>18</sup>F-NaF PET is an inexpensive PET tracer that is already approved for bone cancer imaging and thus this technique could be easily translated to clinical use.

However, in the reported studies, the difference in target-to-background ratio (TBR) between culprit plaques (implicated in AMI) and non-culprit plaques in coronary <sup>18</sup>F-NaF PET is relatively small. The actual values of TBR, generally below 2, even in positive cases, are relatively low. This is primarily due to significant motion of plaques in the coronary vasculature that can be caused by patient cardiac motion (beating of the heart) and respiration. In addition, gross patient motion during the PET scan acquisition can also add to general loss of TBR. This results in images hampered by noise, as illustrated in Figure 1.

The recent general purpose motion-correction methods proposed for PET motion correction<sup>4-6</sup> are not directly applicable to these images, due to a lack of clear anatomical landmarks in the heart region on the <sup>18</sup>F-NaF PET images. The <sup>18</sup>F-NaF activity localizes only in the plaque lesions and there is no activity seen in the myocardium. To partially address the problem of cardiac motion, in the initial clinical <sup>18</sup>F-NaF PET study only one cardiac phase (representing about 25% of the PET data) was used<sup>1</sup>, at the expense of significant noise increase. The noise was increased due to subsampling of the PET acquisition data.

In a recent study<sup>7</sup>, we evaluated the use of non-rigid registration using a level-set algorithm to the segmented coronary arteries to correct for cardiac motion. This allowed an important noise decrease due to the use of all collected counts, as well as a better discrimination between culprit and non-culprit plaques, as compared to the use of only one cardiac phase, as seen in the other studies to date. However, the level-set method that we utilized may not be the most optimal algorithm for this new application. Therefore, in this study, we aimed to also investigate demons method and in its ability to correct cardiac motion of coronary <sup>18</sup>F-NaF PET.

## 2. DATA AND IMAGING PROTOCOL

### Patients

Patients were recruited from the Royal Infirmary of Edinburgh between February, 2012, and January, 2013, in two cohorts: 6 patients with acute ST-segment or non-ST-segment

elevation myocardial infarction<sup>8</sup> and 9 patients with stable angina pectoris undergoing elective invasive coronary angiography. Exclusion criteria were age <50 years, insulin-dependent diabetes mellitus, women of childbearing age not receiving contraception, severe renal failure (serum creatinine >2.8 mg/dL), known contrast allergy, and inability to provide informed consent. All patients underwent a comprehensive baseline clinical assessment, including evaluation of their cardiovascular risk factor profile. Studies were completed with the approval of the local research ethics committee, in accordance with the Declaration of Helsinki, and with the written informed consent of each participant.

### Imaging and Analysis Protocols

All patients underwent cardiac-gated <sup>18</sup>F-NaF PET/CT imaging of the coronary arteries with a hybrid scanner (128-multidetector Biograph mCT, Siemens Medical Systems, Erlangen, Germany). Study subjects were administered a target dose of 125 MBq <sup>18</sup>F-NaF intravenously, and subsequently rested in a quiet environment for 60 min. An attenuation correction CT scan (non-enhanced 120 kV and 50 mA) was then performed, followed by PET imaging of the thorax in list-mode for 20 min.

Prospectively-gated coronary CT angiography (CCTA) was undertaken in the same visit as the <sup>18</sup>F-NaF scan. Depending on the BMI, a bolus of 80-100 mL of contrast (400 mgI/mL; Iomeron, Bracco, Milan, Italy) was injected intravenously at 5 mL/s, after determining the appropriate trigger delay with a test bolus of 20 mL contrast material.

ECG-gated PET images were reconstructed using the Siemens Ultra-HD algorithm in multiple phases of the cardiac cycle. For this study, 2 different sets of data were reconstructed from list mode data: one gate with 25% of the counts during the end-diastolic phase (technique used in the original Joshi et al study<sup>1</sup>) and 10 cardiac-gated bins. The PET pixel size was either  $2 \times 2 \times 2$  or  $4 \times 4 \times 2$  mm. The CCTA scans were reconstructed at  $0.75 \times 0.7$  mm and  $0.6 \times 0.3$  mm for retrospective and prospective acquisitions respectively at 70% of the cardiac cycle.

## 3. METHODOLOGY

### Cardiac motion correction

The goal of the motion correction method was to compensate for coronary artery motion in the different phases of the ECG-gated PET data. Gated PET with 10 time bins were reconstructed from the PET list-mode files. The registration aimed to align all gates to the end-diastolic phase position to compensate for coronary artery motion. It allowed to synchronize the registered data to i) the prospective CCTA and ii) the one gated time-bin of PET data corresponding to the end-diastolic phase, taken as the reference in the original study.

In order to recover the anatomical information that is missing in the PET data, we used the contrast CCTA data that clearly delineates the coronary arteries. The CCTA data were obtained in end-expiration position, which allowed very good alignment with PET data when patient remains in the same position. However, in all cases, verification and manual correction (if needed) of relative CCTA and PET position were performed by an experienced

observer. Coronary regions were first extracted from the CCTA by vessel tracking based on Bayesian maximal paths<sup>9</sup>, as previously implemented and validated in our CCTA processing software<sup>10-12</sup>. The centerlines of the right coronary artery (RCA), left circumflex artery (LCX) and left anterior descending (LAD) coronary artery were extracted for every patient in this manner. The centerline detection required manual identification of the start and end of the vessel but all further detection was fully automatic. Subsequently, the centerline coordinates were transferred to the PET volumes to automatically extract 3D tubular volumes of interest (VOI) surrounding the coronary arteries in the gated PET images. The tubular volumes were defined by a 20-mm radius around each centerline.

Then, two different registration algorithms were applied selectively only to the extracted coronary regions: a nonlinear level-set algorithm<sup>13</sup> and a symmetric log-domain diffeomorphic registration based on demons<sup>14</sup>, for comparison purpose. We used the ITK<sup>15</sup> implementations of both algorithms. Every VOI of the PET data from each gate was then registered to the end-diastolic reference artery region. After the registration process, all the registered VOIs were inserted back in their original PET image. Finally, all registered PET images were summed into one static image volume to obtain 10-gate cardiac motion-corrected PET data based on the level-set and demons registration algorithms. An illustration of the motion correction method is given in Figure 2.

### Lesion and measures definitions

To define the lesions, PET data were fused with the CCTA, and analyzed by experienced observers blinded to the clinical diagnosis using OsiriX 6.5 workstation software on an Apple computer. Two dimensional regions of interest were drawn around all major epicardial vessels (diameter >2 mm) on 3-mm axial slices just beyond the discernible adventitial border. We used a previously established 95% lower reference limit to categorize coronary plaques into <sup>18</sup>F-NaF positive and negative lesions, on the end-diastolic data as in the original study<sup>1</sup>. In the fifteen patients, 23 positive and 21 negative lesions were delineated in this manner.

TBR measurements were defined as the ratio between the maximum activity values in the manually defined lesion over the mean value of the background, which was taken as the blood pool in the middle of the left ventricle (also manually defined). The noise level was determined as the ratio of the mean over the standard deviation of the background and expressed as percentage.

Two methods were then used to evaluate the motion found by the two registration algorithms: 1) the maximal motion that was detected in any of the 3 arteries of interest (LAD, LCX and RCA) during the registration process, and 2) the singularities in the deformation field. The maximal motion was computed as the maximal deformation field vector amplitude (in mm) for each patient in every coronary vessel and then averaged over the 15 patients. The measurement of absolute motion allows us to determine how realistic these deformation fields were as compared to physiologically known values. On the other hand, singularities reflect how physically plausible the registration deformation is: we expect that a deformation should be bijective, i.e. define a one-to-one correspondence between points in the fixed and in the moving image. Regions where the deformation field is not

bijjective are commonly referred to as singularities. We thus calculated the determinant of the Jacobian of the deformation field at every point<sup>16</sup>. Every point with a Jacobian = 0 denotes a singularity. The overall error is given by the percentage of points with a singularity.

### Statistical analysis

Statistical analyses were performed with Analyse-it 2.26 software. Non-parametric results were presented as median and inter quartile range (IQR) and compared using the Wilcoxon signed-rank test as appropriate. A two-sided  $p < 0.05$  was taken as statistically significant.

## 4. RESULTS

### Comparison of TBR and Noise

<sup>18</sup>F-NaF activity ratio between lesion and background (expressed as TBR) in the positive lesions, as compared to diastolic image data, was 4% higher (1.82 [IQR 1.54-2.18] *vs* 1.75 [IQR 1.59-2.15],  $p=0.9$ ) with the demons motion registered data and 11% higher (1.94 [IQR 1.64-2.34] *vs* 1.75 [IQR 1.59-2.15],  $p=0.05$ ) with the level-set motion registered data. In <sup>18</sup>F-NaF negative lesions, we observed a similar activity for level-set or demons motion registered data as compared to diastolic image data: 0.90 [IQR 0.80-1.0] for level-set *vs* 0.90 [IQR 0.70-0.99],  $p=0.07$  and 0.87 [IQR 0.78-0.92] for demons *vs* 0.90 [IQR 0.70-0.99],  $p=0.66$ ). Overall, the median TBR difference between <sup>18</sup>F-NaF positive and negative lesions increased from 0.85 to 0.95 using the demons method and even to 1.04 using the level-set algorithm, as compared to one gate ( $p < 0.05$ ). Both methods should therefore allow for a better discrimination between positive and negative lesions, as compared to the single end-diastolic gate alone that was presented in the original trial<sup>1</sup>.

Noise was significantly reduced by using the level-set motion registration as compared to the single end-diastolic gate: 0.11 [IQR 0.08-0.12] *vs* 0.18 [IQR 0.15-0.23],  $p < 0.0001$ . It was even further reduced for the demons registration 0.09 [IQR 0.08-0.12] *vs* 0.18 [IQR 0.15-0.23],  $p < 0.0001$ ). This is an expected finding since only a subset of the PET counts was used in the one end-diastolic cardiac bin of data, while all the counts were used for level-set and demons motion-corrected data.

### Evaluation of Motion Extent and Smoothness

First, we computed the extent of motion for all 15 patients. With the demons registration, the median end-systolic to end-diastolic displacement was 17.2 mm [IQR 14.6-19.0 mm] in the LAD, 17.7 mm [IQR 16.1-20.7 mm] in the LCX and 19.4 mm [IQR 16.2-22 mm] in the RCA. Results obtained with level-set data were higher: the displacement was 32.9 mm [IQR 29.7-36.4 mm] in the LAD, 30.1 mm [IQR 28.3-31.5 mm] in the LCX and 33.0 mm [IQR 30.8-39.8 mm] in the RCA. The results for demons are in accordance with the expected range of the maximal coronary motion during the cardiac cycle that has been reported in the literature<sup>17, 18</sup>, while the results obtained with level-set registration are much higher than what has been physiologically observed. This can be explained by some abrupt changes in the deformation field that occur at the border between the registered volume of interest (VOI) and the non-registered original PET image with the level-set procedure, as illustrated

in Figure 3. On the opposite, demons method preserves continuity between the registered and non-registered VOI, ensuring a smooth transition between both regions.

Singularities represent 8% of the voxels in the RCA, 4% of the voxels in the LAD and 7% of the voxels in LCX for the level-set method, while none of the voxels present a singularity using the demons. This suggests that demons registration produces more realistic deformations.

## 5. NEW OR BREAKTHROUGH WORK TO BE PRESENTED

This work presents the first comparison of registration algorithms for the purpose of correcting the motion of  $^{18}\text{F}$ -sodium fluoride PET data, using CCTA's anatomical framework. This may enable a wide use of this novel imaging technique for early detection of coronary artery diseases.

This work has not been submitted elsewhere.

## 6. CONCLUSION

Cardiac motion correction of gated  $^{18}\text{F}$ -NaF PET/CT reduces noise and increases TBR as compared to end-diastolic gate imaging, and hence tends to allow a better discrimination between positive and negative lesions. The demons method produces smoother deformation fields as compared to the level-sets method, with a motion that is physiologically plausible. Therefore, level-set technique will likely require additional post-processing steps. On the other hand, the observed TBR increases were the highest for the level-set technique. Furthermore, the incorporation of the CCTA's anatomical framework, as proposed here, can lead to automation and reproducibility of quantitative analysis of PET uptake. Further investigations of the optimal registration technique of this novel coronary PET imaging technique are warranted.

## ACKNOWLEDGMENTS

This study was supported in part by a grant (*Cardiac Imaging Research Initiative*) from the Adelson Medical Research Foundation. This research was also supported in part by grant R01HL089765 from the National Heart, Lung, and Blood Institute/National Institutes of Health (NHLBI/NIH) (PI: Piotr Slomka). Its contents are solely the responsibility of the authors and do not necessarily represent the official views of the NHLBI.

## REFERENCES

1. Joshi NV, Vesey AT, Williams MC, et al.  $^{18}\text{F}$ -fluoride positron emission tomography for identification of ruptured and high-risk coronary atherosclerotic plaques: a prospective clinical trial. *Lancet*. 2014; 383(9918):705–13. [PubMed: 24224999]
2. Dweck MR, Chow MW, Joshi NV, et al. Coronary arterial  $^{18}\text{F}$ -sodium fluoride uptake: a novel marker of plaque biology. *Journal of the American College of Cardiology*. 2012; 59(17):1539–1548. [PubMed: 22516444]
3. Irkle A, Vesey A, Lewis D, et al. Identifying active vascular microcalcification by  $^{18}\text{F}$ -sodium fluoride positron emission tomography. *Nature Communications*. 2015; 6(7495)
4. Gigengack F, Ruthotto L, Burger M, et al. Motion correction in dual gated cardiac PET using mass-preserving image registration. *IEEE Trans Med Imaging*. 2012; 31(3):698–712. [PubMed: 22084048]

5. Lamare F, Le Maitre A, Dawood M, et al. Evaluation of respiratory and cardiac motion correction schemes in dual gated PET/CT cardiac imaging. *Medical physics*. 2014; 41(7):072504. [PubMed: 24989407]
6. Hong, I.; Jones, J.; Casey, M. Elastic motion correction for cardiac PET studies. *IEEE*; 2013.
7. Rubeaux M, Joshi NV, Dweck MR, et al. Motion Correction of <sup>18</sup>F-NaF PET for Imaging Coronary Atherosclerotic Plaques. *Journal of Nuclear Medicine*. 2016; 57(1):54–59. [PubMed: 26471691]
8. Thygesen K, Alpert JS, Jaffe AS, et al. Third universal definition of myocardial infarction. *Glob Heart*. 2012; 7(4):275–95. [PubMed: 25689940]
9. Lesage, D.; Angelini, ED.; Bloch, I., et al. [Bayesian maximal paths for coronary artery segmentation from 3D CT angiograms]. Springer; 2009.
10. Schuhbaeck A, Dey D, Otaki Y, et al. Interscan reproducibility of quantitative coronary plaque volume and composition from CT coronary angiography using an automated method. *Eur Radiol*. 2014; 24(9):2300–8. [PubMed: 24962824]
11. Dey D, Achenbach S, Schuhbaeck A, et al. Comparison of quantitative atherosclerotic plaque burden from coronary CT angiography in patients with first acute coronary syndrome and stable coronary artery disease. *J Cardiovasc Comput Tomogr*. 2014; 8(5):368–74. [PubMed: 25301042]
12. Diaz-Zamudio M, Dey D, Schuhbaeck A, et al. Automated Quantitative Plaque Burden from Coronary CT Angiography Noninvasively Predicts Hemodynamic Significance by using Fractional Flow Reserve in Intermediate Coronary Lesions. *Radiology*. 2015:141648. in press.
13. Vemuri BC, Ye J, Chen Y, et al. Image registration via level-set motion: Applications to atlas-based segmentation. *Medical image analysis*. 2003; 7(1):1–20. [PubMed: 12467719]
14. Vercauteren, T.; Pennec, X.; Perchant, A., et al. [Symmetric log-domain diffeomorphic registration: A demons-based approach]. Springer; 2008.
15. Ibáñez, L.; Schroeder, W.; Ng, L., et al. *The ITK Software Guide*. Kitware; 2003.
16. Rey D, Subsol G, Delingette H, et al. Automatic detection and segmentation of evolving processes in 3D medical images: Application to multiple sclerosis. *Med Image Anal*. 2002; 6(2):163–79. [PubMed: 12045002]
17. Shechter G, Resar JR, McVeigh ER. Displacement and velocity of the coronary arteries: cardiac and respiratory motion. *IEEE Trans Med Imaging*. 2006; 25(3):369–75. [PubMed: 16524092]
18. Wang Y, Vidan E, Bergman GW. Cardiac Motion of Coronary Arteries: Variability in the Rest Period and Implications for Coronary MR Angiography I. *Radiology*. 1999; 213(3):751–758. [PubMed: 10580949]

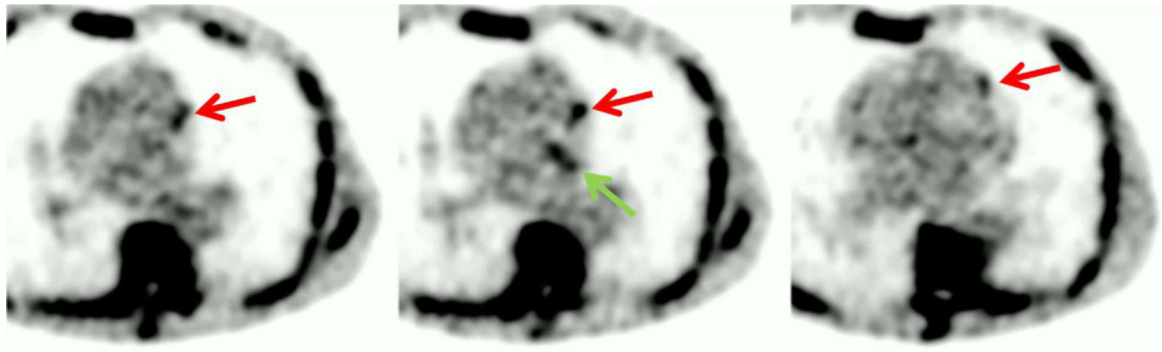


**Figure 1.**

Example of one time bin from 10 gates  $^{18}\text{F}$ -NaF raw data. Positive tracer uptake can be seen in the left circumflex artery (LCX-green arrow) and left anterior descending (LAD-red arrows) coronary arteries.

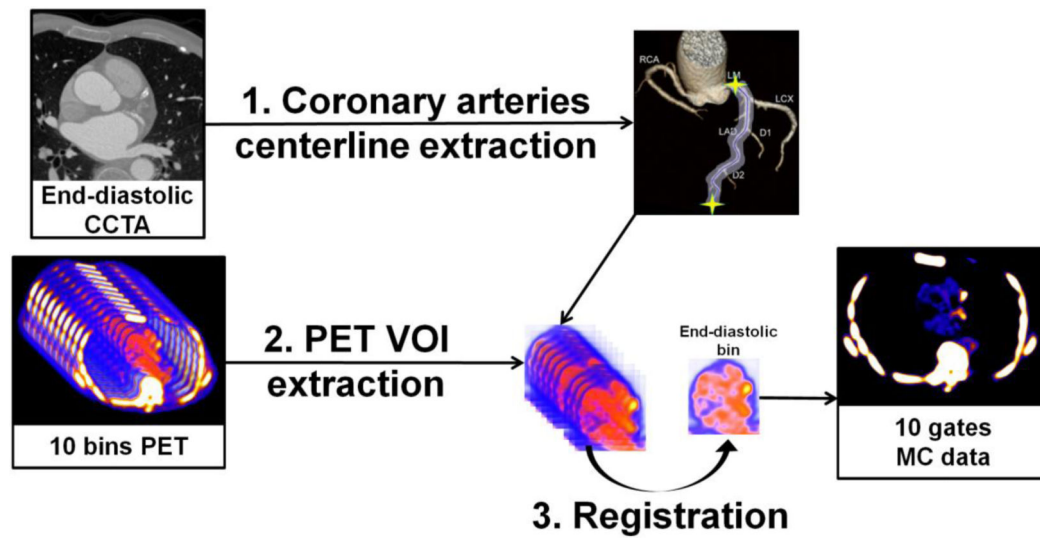


**Figure 2.**

Overview of the motion correction method. (1) Coronary artery centerlines are extracted from CCTA in end-diastolic phase (2) Volumes of interest (VOIs) surrounding coronary arteries are extracted from 10-bin PET data using previously extracted CCTA centerlines. (3) All bins of data are registered to common end-diastolic reference bin by nonlinear level-set or demons registration restricted to coronary regions. Then, registered VOIs are inserted back into their original PET volumes, and all registered PET images are summed into a single volume to obtain motion-corrected 10-bin data. MC = motion-corrected; VOI = volume of interest.

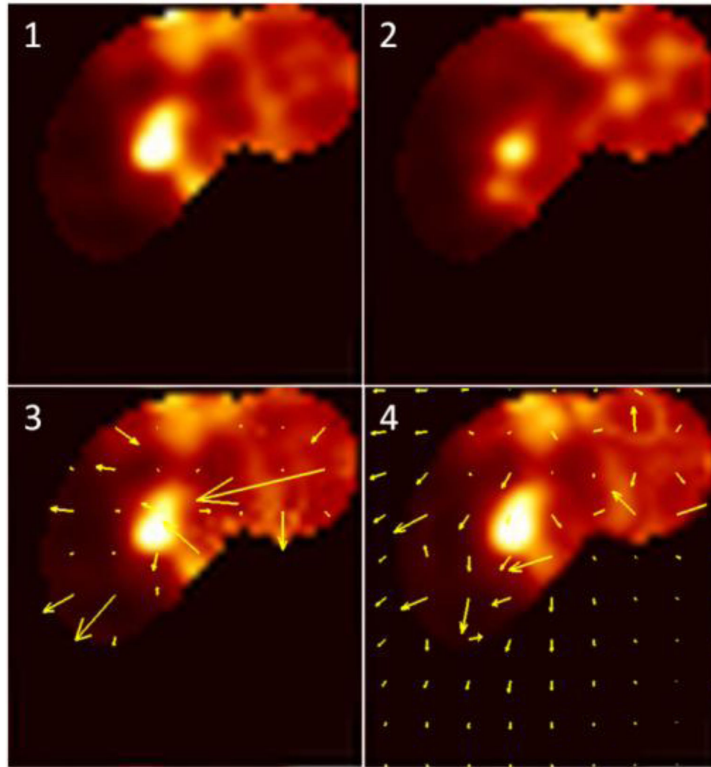


**Figure 3.**

Example. PET volume of interest registration to end diastolic position in the of Left Anterior Descending (LAD) coronary artery region. (1) Reference end diastolic (7<sup>th</sup> time bin) PET image. (2) An example of a floating (3<sup>rd</sup> time bin) PET image. (3) Level-set registered gate 3 with overlaid deformation field. (4) Demons registered gate 3 with overlaid deformation field. For each patient, 9 such registrations needed to be performed to register each of the floating gates to the end-diastolic reference gate.